THERMOHYDRAULIC ANALYSIS OF TWO-PHASE CAPILLARY PUMPING SYSTEMS FOR INDUSTRIAL DESIGN AND SPACE APPLICATIONS

Paulo Henrique Dias dos Santos
Federal University of Santa Catarina, Departament of Mechanical Engineering
LabCET - Laboratory of Combustion and Thermal Systems Engineering
Campus Universitário, 88.040-900, Florianópolis, SC, Brazil
paulosantos@labcet.ufsc.br

Edson Bazzo
Federal University of Santa Catarina, Departament of Mechanical Engineering
LabCET - Laboratory of Combustion and Thermal Systems Engineering
Campus Universitário, 88.040-900, Florianópolis, SC, Brazil
ebazzo@emc.ufsc.br

Abstract. *Capillary pumping systems are two-phase heat transfer loops that have been currently in development. They are used in aerospace applications and in refrigeration systems in general. These highly efficient heat transfer devices work in a range of operation temperature, usually defined by the working fluid properties. The working fluid circulation is accomplished by the capillary forces action generated in the wick of the evaporation zone into the evaporator. Therefore, the pumping mechanism does not consume electric power. This paper presents an introduction to the thermohydraulic study in regarding to the CPL/LHP design, in order to develop a combined device that simultaneously associates the advantages of CPL (operation temperature control of the system) and LHP (robustness and no heating precondition during the start-up), looking for more flexibility and increasing the system reliability. In this paper are presented the fixed and variable conductance modes and the Pressure-Temperature diagrams for CPL/LHP. It is also shown an analysis for the choice of the working fluid by the figure of merit, as well as the influence of the subcooling as a function of the saturation curve slope and the pressure losses of a typical example of capillary pumping system with cylindrical evaporator.*

Keywords*: Capillary pumping systems, Capillary evaporator, CPL, LHP.*

1. INTRODUCTION

CPL (Capillary Pumping Loop) and LHP (Loop Heat Pipe) are two-phase heat transfer loop systems that have been currently in development. They are used in aerospace applications and in refrigeration systems in general. These highly efficient heat transfer devices work in a range of operation temperature, usually defined by the working fluid properties. The working fluid circulation is accomplished by the capillary forces action generated in the wick of the evaporation zone into the evaporator. Therefore, the pumping mechanism does not consume electric power.

The working fluid choice involves several factors associated to the operation, availability and safety. The ammonia is frequently used in capillary pumping systems by presenting physical properties more favorable. But other working fluids present good operation such as: water, ethanol, acetone, propylene, methanol, butane, isobutene and propane. The operation temperature range constitutes the preliminary condition for the selection of the possible thermal fluids for certain application. This range is between the triple and critical points, because below the triple point and above the critical point there is no circulation of the thermal fluid.

The capillary pumping capacity depends on the surface tension of the working fluid and the wick used. Nowadays, the classification of the operational fluids has only been made according to the capillary limit that is function of the pressure losses in the system. Therefore the knowledge of the flowing state is very important for the design of the capillary pumping systems. There exist another limit called boiling limit presented by these systems, but for lack of knowledge of this limit, the fluids that present this problem have been avoided.

For determining the flowing states in each system component it makes necessary the understanding of its thermodynamic behavior. It should be focused special attention upon the heat transfer processes related to the sensible heat part of these systems, that corresponds to the liquid subcooling in the condenser outlet. The processes involved in the fluid evaporation, in the feeding channel of the evaporator wick and/or in the liquid return line of the condenser, need a good thermodynamic knowledge.

Ku (1994) was the first to publish a real conditions evaluation of CPL operation, basing his analysis on the PT diagram. The conclusions in theoretical base, justified the high needed of subcooling presented by some working fluids. A similar analysis, through the PT diagram, was also published for LHP by Maidanik et al. (1991), Ku (1999) and Maidanik (2004).

The operation modes of the capillary pumping systems can be classified as: fixed or variable conductance. In the variable conductance mode, the system saturation temperature can be controlled even so thermal load varies. On the other hand in the fixed conductance mode, the greater the thermal load, the greater the system saturation temperature. Nikitkin and Cullimore (1998) presented qualitative graphs of the vapor temperature profile for CPL and LHP operating in the fixed and variable conductance modes. While Chernysheva et al. (2007) just presented quantitative graphs for LHP.

This paper presents an introduction to the thermohydraulic study in regarding to the CPL/LHP design, in order to develop a combined device that simultaneously associates the advantages of CPL (operation temperature control of system) and LHP (robustness and no heating precondition during the start-up), looking for more flexibility and increasing the system reliability. In this paper are presented the fixed and variable conductance modes and the Pressure-Temperature diagrams for CPL/LHP. It is also shown an analysis for the choice of the working fluid by the figure of merit, as well as the influence of the subcooling as a function of the saturation curve slope and the pressure losses of a typical example of capillary pumping system with cylindrical evaporator.

2. OPERATION MODES

2.1. Fixed Conductance

The operation modes of the capillary pumping systems can be classified as: fixed or variable conductance. Fig. 1 depicts a typical fixed conductance CPL. This device is composed of an evaporator, a condenser, a subcooler and liquid and vapor transport lines. A working fluid evaporates when heated into the evaporator and condenses when cooled into the condenser. The evaporator possesses a wick that promotes the working fluid circulation in the loop. The fluid circulation occurs in a continuous way and in a same direction, differently of the circulation in the heat pipe, where the liquid and the vapor flow in opposite directions.

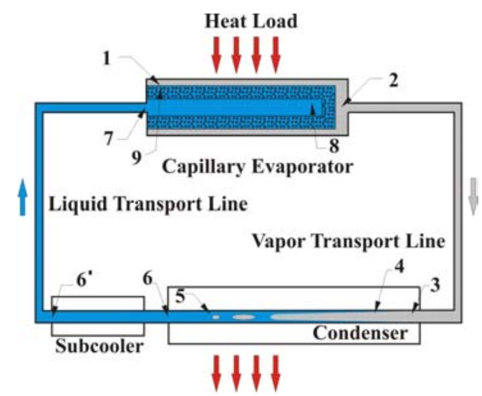

Figure 1. Functional schematic of a fixed conductance CPL.

Fixed conductance CPL operates in the following manner: heat is supplied to the evaporator so that the liquid saturated into the wick evaporates, forming at the same time the menisci in the interface liquid-vapor, that promote the fluid circulation through the capillary forces developed by the fluid surface tension. The vapor generated in the evaporator goes via vapor transport line to the condenser, where heat is removed and the vapor condenses. The fluid is subcooled before coming back to the evaporator so that no vapor bubble migrates to the evaporator.

Fixed conductance CPLs have as characteristics: (i) the subcooler is usually an integral part of the condenser; (ii) they do not possess reservoir that serves as a fluid accumulator; (iii) the vapor condensation area in the condenser remains constant as the thermal load varies; (iv) the system operation temperature is dependent on the thermal load, supplied to the evaporator, and on the condenser sink temperature.

The maximum capillary pressure head ($\Delta P_{cap,max}\ [Pa]$) is function of the fluid surface tension ($\sigma\ [N/m]$), the effective pumping radius of the wick ($r_P\ [m]$) and the contact angle between the liquid and the vapor phase ($\theta = 1°$):

$$\Delta P_{cap,max} = \frac{2\sigma \cos\theta}{r_P} \tag{1}$$

The CPL operation requires that the sum of the pressure drops in the components and in the transport lines must be smaller than the maximum capillary pressure head developed by the wick:

$$\Delta P_{cap,max} \geq \Delta P_{evap} + \Delta P_{cond} + \Delta P_v + \Delta P_l + \Delta P_g \tag{2}$$

In Eq. (1) is noticed that the maximum capillary pressure head is just function of the fluid surface tension, the contact angle and the pore radius size. However, on the right side of Eq. (2), is noticed that the pressure losses depend on the system design and the power input to the evaporator. In the normal operation of a CPL, the menisci formed in the liquid-vapor interfaces are naturally adjusted to establish a capillary pumping head that matches the suffered pressure losses in the components and in the transport lines. When the total pressure loss in the system exceeds the maximum capillary pressure head, vapor will penetrate in the wick causing the dryout and blocking the liquid inlet. In case it happens the system will fail.

A PT diagram is depicted in Fig. 2 for better understanding the phenomena that happens in CPL shown in Fig. 1. In order to simplify the discussion is assumed that the system transport lines are insulated. In the point 1, the liquid vaporizes at a saturation temperature T_1 corresponding to a pressure P_1. The generated vapor flows via the evaporator grooves causing a pressure drop due to the viscous friction from P_1 to P_2, in a close location of the evaporator outlet, where liquid vaporizes at a lower saturation temperature $T_2^{'}$. Therefore, the liquid vaporizes along the external wick surface at a temperature range between T_1 and $T_2^{'}$, instead of a fixed temperature T_1. The vapor leaves the evaporator in the superheated state (point 2) partly due to the decrease in the saturation pressure and partly due to the proximity of the hot source that supplies the system. The vapor continues to lose pressure as flows via vapor transport line. Between the points 2 and 3, the vapor experienced an adiabatic expansion process and its temperature decreases lightly.

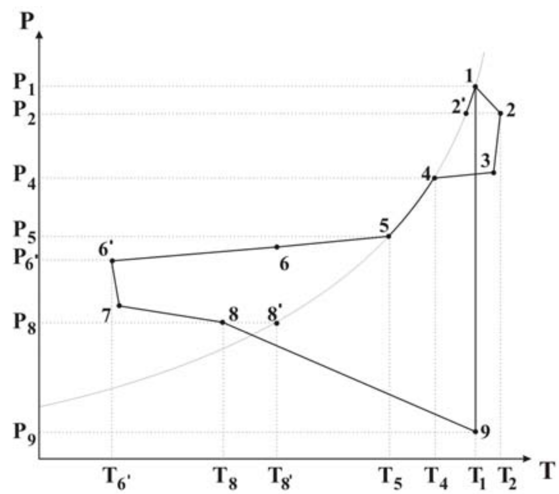

Figure 2. PT diagram for a fixed conductance CPL.

The vapor thermodynamic state that enters in the condenser is represented by the temperature T_3 and pressure P_3. According to Ku (1994) a small area of the condenser is enough to dissipate the sensible heat before the beginning of the vapor condensation in the point 4 at a pressure P_4 (smaller than P_3) and at a saturation temperature T_4.

The vapor condensation happens between the points 4 and 5. In the point 5 there is no more vapor. Similar to the liquid vaporization into the evaporator, the vapor condensation occurs at a temperature range between T_4 e T_5. The liquid continues to lose sensible heat up to reach a subcooled temperature T_6 in the condenser outlet. A further subcooling is necessary to ensure that no vapor bubble goes to the evaporator. Therefore the liquid goes by the subcooler and leaves it in a subcooling state to the temperature $T_6^{'}$. The liquid temperature increases lightly, while the pressure decreases from $P_6^{'}$ to P_7 in the liquid feeding channel inlet of the evaporator. Inside the feeding channel, the liquid is heated until a temperature T_8. This heating is due to the heat leak from the wick to the fluid.

The point $8^{'}$ represents the saturation state corresponding to the pressure P_8. The liquid in the external wick surface is heated and reaches the saturation temperature T_1 corresponding to the pressure P_1 before vaporizing. It is noticed by Fig. 2 that the liquid side of the menisci (point 9) is in its superheated state. The total pressure drop in the system is equal to the difference between P_1 and P_9 which in its turn cannot be larger than the maximum capillary pressure head.

According to Ku (1999), in the most of the two-phase capillary pumping systems the changes of pressure and temperature are extremely small; therefore it can approach the saturation curve for a straight line between two points using the Clausius-Clapeyron equation:

$$\left.\frac{dP}{dT}\right|_{T_{sat}} = \frac{h_{lv}}{T_{sat} v_{lv}} \tag{3}$$

where: $\left.\frac{dP}{dT}\right|_{T_{sat}}$ is the slope of the pressure-temperature saturation line *[Pa/K]*, h_{lv} is the latent heat of vaporization $[kJ/kgK]$, T_{sat} is the saturation temperature *[K]* e v_{lv} is the difference in specific volumes during vaporization *[m³/kg]*.

According to Maidanik et al. (1991), taking for instance the points 1 and 4, the saturation line slope times the temperature differential between these two points of the curve is approximately equal to the pressure differential between them:

$$\left.\frac{dP}{dT}\right|_{T_4}(T_1 - T_4) \simeq (P_1 - P_4) \tag{4}$$

In Eq. (4), is noticed that the decrease in the temperature is directly proportional to the pressure drop between the points 1 and 4. This pressure drop is function of the mass flow rate which in its turn is function of the power input to the evaporator.

According to Ku (1994), the heat transfer rate by vaporization is the same that by condensation ($\dot{Q}_{cond} = \dot{Q}_{evap}\ [W]$). The heat transfer rate in the condenser can be expressed as:

$$\dot{Q}_{cond} = h_{cond} A_{cond} (T_4 - T_0) \tag{5}$$

where: h_{cond} is the heat transfer coefficient *[W/m²K]* and A_{cond} is the heat transfer area *[m²]* in the condenser.

For a CPL with fixed liquid volume, the thermal conductance ($h_{cond} A_{cond}$) remains constant. For a given heat transfer rate rejected by the condenser ($\dot{Q}_{cond}$) and a condenser sink temperature T_0, the vapor in the condenser will condense at the temperature T_4 in agreement with Eq. (5) and the liquid will vaporize in the evaporator at the temperature T_1 in agreement with Eq. (4).

Any change in the input heat to the evaporator and/or in the condenser sink temperature will result in changes of the T_1 and T_4. Therefore, the main characteristic of a fixed conductance CPL is its strongly dependence on the operation temperature with regard to the input heat and to the condenser sink temperature.

2.2. Variable Conductance

In a variable conductance CPL, a reservoir will be included. The reservoir function is to control the operation temperature of the system and to accumulate the liquid excess that is not being required in the loop.

Analyzing Eq. (5), can be understood how works the variable conductance mechanism. If the condenser sink temperature T_0 remains constant and the system thermal load increases, more vapor will be generated in the evaporator and the vapor excess will accumulate in the condenser, causing a local pressure increase. This pressure increase which in its turn causes a liquid displacement from the condenser to the reservoir, as it can be seen in Fig. 3. This happens because the condensation temperature T_4 remains constant and the heat transfer area A_{cond} increases so that Eq. (5) is satisfied.

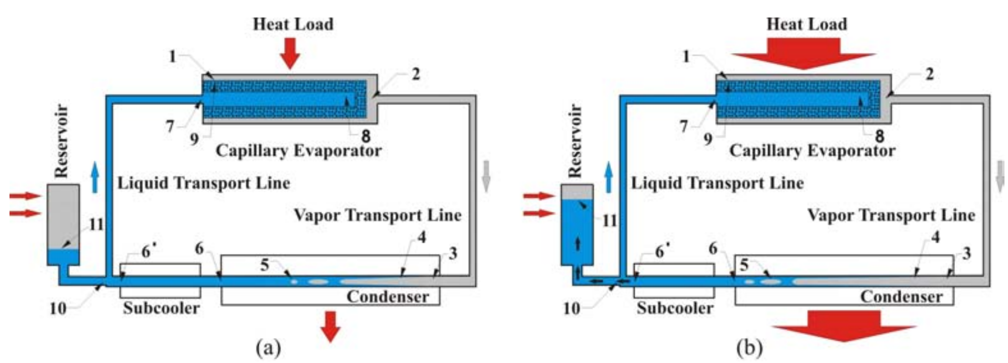

Figure 3. Functional schematic of a variable conductance CPL.

In case the system thermal load decreases and T_0 remains constant, the vapor pressure into the condenser will decrease. An unbalance in the pressure between the reservoir and the condenser will force the liquid displacement from the reservoir to the condenser, reducing the heat transfer area A_{cond} automatically so that Eq. (5) is satisfied. Similar analysis can be made varying the condenser sink temperature T_0.

The Fig. 4 depicts a PT diagram for a variable conductance CPL, shown in Fig. 3. The point 11 corresponds to the saturation state into the reservoir. In any circumstance, the vapor condensation temperature T_4 is related to the reservoir saturation temperature T_{11} by the union of Eqs. (3 and 4):

$$(T_4 - T_{11}) = \frac{(P_4 - P_{11})T_{11}v_{lv}}{h_{lv}} \tag{6}$$

The PT diagram is developed for steady state; therefore there is no mass flow between the loop and the reservoir. The only pressure gradient possible between the points 10 and 11 is due to the hydrostatic pressure. The other points are similar to the ones showed in Fig. 2.

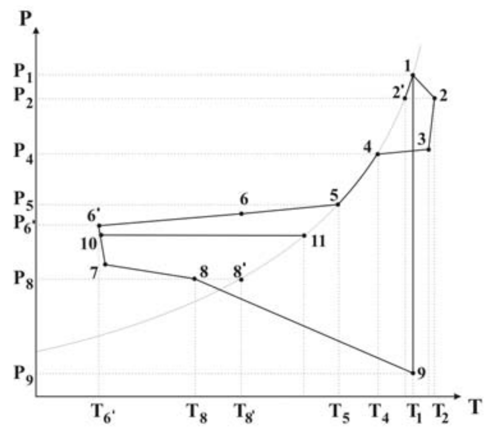

Figure 4. PT diagram for a variable conductance CPL.

The variable conductance CPL, shown in Fig. 3, operates in the following manner: before the system startup, the condenser is submitted to the temperature T_0 and the reservoir is heated up to temperature T_{11} (which is higher than the temperatures of the rest of the loop). Then, the thermal load is supplied to the evaporator. As the evaporator is heated up to the same temperature T_{11} or lightly superior to the one, the liquid is vaporized and the menisci formed in the wick force the vapor flowing to the condenser via vapor transport line. An equilibrium condition will be established in the condenser so that the vapor condenses at the temperature T_4 that is very close to the reservoir temperature T_{11}. An equilibrium condition will also be established in the evaporator so that the liquid vaporizes to the temperature T_1.

The condensation temperature T_4 is not sensitive nor to the changes in the condenser sink temperature T_0, much less to the changes in the system thermal load. Therefore, the temperature T_4 is controlled by the reservoir saturation temperature T_{11}.

LHP is a type of variable conductance CPL and was developed to supply the apparent disadvantage of CPL in the needed of pre-heating during the startup. In LHP, the reservoir, also denominated hydro-accumulator or compensation chamber which has capillary connection with the evaporator, ensures the liquid presence in the evaporator wick. A secondary wick usually connects the compensation chamber to the evaporator. The compensation chamber is located close to the evaporator, usually in the capillary pumping inlet as it can be seen in Fig. 5; or taking the place of what would be the liquid feeding channel of the evaporator. Thereby, in a LHP the liquid reservoir presents direct thermal contact with the evaporator (hot source), differently of CPL where it is connected to the condenser (cold source).

The Fig. 6 depicts a PT diagram for variable conductance LHP, shown in Fig. 5. The point 10 corresponds to the saturation state into the compensation chamber.

In any circumstance, the liquid vaporization temperature T_1 is related to the saturation temperature of the compensation chamber T_{10} by the union of Eqs. (3 and 4):

$$(T_1 - T_{10}) = \frac{(P_1 - P_{10})T_{10}v_{lv}}{h_{lv}} \tag{7}$$

The PT diagram, shown in Fig. 6, presents an analysis for steady state; therefore there is no mass flow between the compensation chamber and the liquid feeding channel of the evaporator. Consequently, the saturation pressure P_{10} in the compensation chamber should be the same pressure P_7.

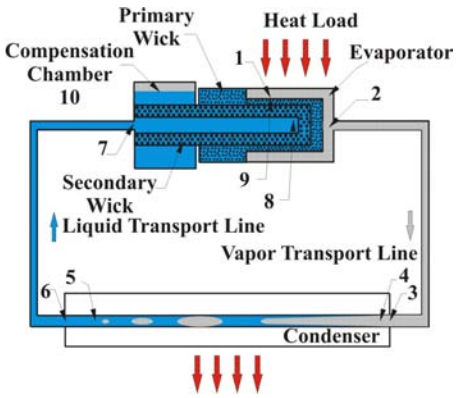

Figure 5. Functional schematic of a LHP.

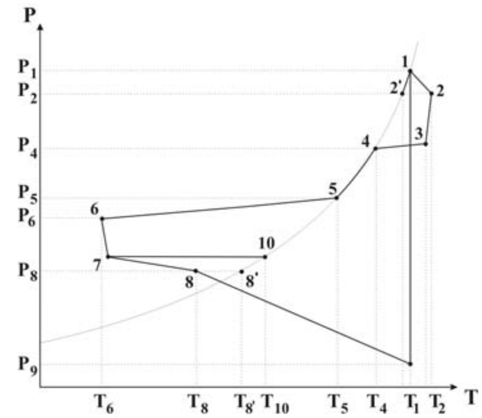

Figure 6. PT diagram for a LHP.

The capillary pumping systems in the variable conductance mode (CPL and LHP shown in Figs. 3 and 5) can work in a binary operation mode. When these systems are operating in a low thermal load condition, the reservoir (CPL) or the compensation chamber (LHP) are operating in the two-phase condition. As it was already mentioned, when the thermal load increases, the condensation front moves forward, causing the liquid displacement from the condenser to the reservoir (CPL) or to the compensation chamber (LHP). Therefore, as the thermal load increases, these compartments will be filled out by the liquid in excess and there will be no more two-phase condition. The evaporation temperature control is only possible if the liquid compartment of the system is in two-phase condition. Consequently, if the thermal load increases up to whole filling of the reservoir (CPL) or the compensation chamber (LHP), the saturation temperature control of the system cannot be made.

Fig. 7 shows qualitatively how is the evaporation temperature profile as a function of the thermal load of CPL and LHP that work in the binary operation mode (fixed and variable conductance).

Fig. (7a) depicts that the evaporator temperature of CPL remains constant in the variable conductance operation mode and starts to increase linearly in the fixed conductance mode. While for LHP, Fig. (7b), even operating in the variable conductance operation mode the evaporator temperature does not remain constant. LHP possesses a range of the evaporation temperature control in the variable conductance mode. This phenomenon happens, according to Chernysheva et al. (2007), due to two factors: (i) decreasing of the condensation area, caused by the liquid displacement from the condenser to the compensation chamber; (ii) changing in the saturation temperature into the compensation chamber T_{11}, that influences directly in the change of the evaporation temperature, due to a complex process of heat and mass transfer. This process happens between the evaporator and the compensation chamber.

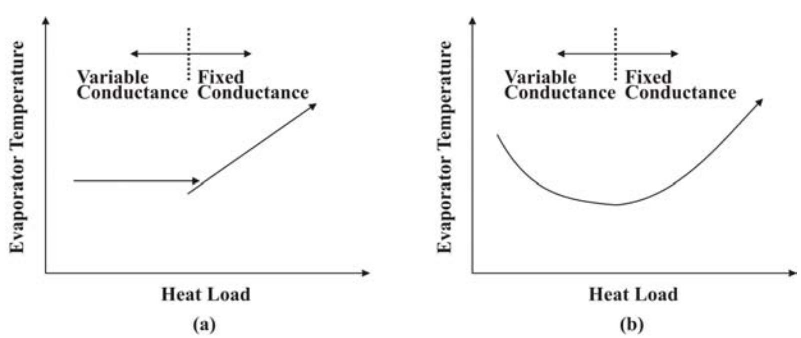

Figure 7. Typical curves of operation for CPL (the) and for LHP (b) in the fixed and variable conductance (Nittkin and Cullimore, 1998).

These above analyses were done in order to develop a combined device that simultaneously associates the advantages of CPL and LHP, looking for more flexibility and increasing the system reliability.

3. PRESSURE LOSSES IN THE CAPILLARY PUMPING SYSTEM

In the capillary pumping systems, the pressure losses in the loop are divided as: in the evaporator ΔP_{evap}, in the condenser ΔP_{cond}, in the transport lines of liquid ΔP_l and vapor ΔP_v. Since this analysis is just made in order to identify which pressure losses have the main influence in design of these systems, the pressure losses in the tubing curves will be neglected because they do not present a certain importance when compared to the other pressure losses. The grooves have also been assumed to be square, i.e., the angle is small negligibly. The Table 1 presents the geometric characteristics of a typical example of capillary pumping system with cylindrical evaporator.

Table 1. Geometric characteristics of a typical example of capillary pumping system with cylindrical evaporator.

Evaporator		***Liquid line***	
Active length (m)	0.6	Diameter (outer/inner) mm	6.35/4.35
Diameter (outer/inner) mm	19.0/12.7	Length (m)	1
Grooves		***Vapor line***	
Number of grooves	12	Diameter (outer/inner) mm	6.35/4.35
Grooves height/width (mm)	2/2	Length (m)	1
Wick of Polyethylene		***Condenser***	
Permeability (m^2)	10^{-12}	Active length (m)	0.6
Diameter (outer/inner) mm	12.7/7.0	Diameter (outer/inner) mm	6.35/4.35

The pressure loss is function of the mass flow rate and, therefore, of the heat input to the evaporator which in its turns includes the latent and sensible heat. The liquid is heated from the subcooling temperature (in the subcooler outlet) up to the evaporation temperature (in the external wick surface). The mass flow rate can be calculated by energy balance in the evaporator:

$$\dot{Q}_{evap} = \dot{m}\, h_{lv} + \dot{m}\, c_p\ \Delta T_{subcooled} \tag{9}$$

where: $\dot{m}$ is the mass flow rate *[kg/s]*, c_p is the liquid specific heat *[J/kgK]* e $\Delta T_{subcooled}$ is the liquid subcooling *[K]*.

The pressure losses in the transport lines of liquid and vapor, in the liquid feeding channel and in the grooves can be estimated using the Eqs. (10 a, b and c), published by Chi (1976):

$$\Delta P = \frac{64}{Re}\frac{\rho V^2 L}{2d} \quad if \quad Re < 2300 \tag{10a}$$

$$\Delta P = \frac{0.31}{Re^{0.25}}\frac{\rho V^2 L}{2d} \quad if \quad 2300 \le Re \le 20{,}000 \tag{10b}$$

$$\Delta P = \frac{0.184}{Re^{0.2}}\frac{\rho V^2 L}{2d} \quad if \quad Re > 20{,}000 \tag{10c}$$

where: *Re* is the Reynolds number [$\rho Vd / \mu$], ρ is the density *[kg/m³]*, *V* is the flowing velocity *[m/s]*, *L* is the effective length *[m]* and *d* is the tube diameter *[m]*.

According to Ku and Kroliczek (1987), both flowing states, laminar or turbulent, can exist in each component of the capillary pumping system, except for the liquid flowing through the evaporator wick, where the laminar flowing state is assumed. For a laminar flowing state through the wick, according to the Darcy's Law, the pressure loss can be calculated by Eq. (11):

$$\Delta P = \frac{\nu_l\, \dot{m}\, ln\left(r_{out} / r_{in}\right)}{K h_{lv} 2\pi L} \tag{11}$$

where: ν_l is the kinematic viscosity of the liquid *[m²/s]*, r_{out} is the outer radius of the wick *[m]*, r_{in} is the inner radius of the wick *[m]* e *K* is the permeability of the wick *[m²]*.

Neglecting compressibility effects of flowing and considering that the void fraction is constant along the length, the pressure drop in the condenser is calculated by Eq. (12), obtained in Carey (1992):

$$\Delta P_{cond} = \phi_{lo}^2 \left(\frac{2 f_{lo} G^2}{\rho_l d_{cond}}\right) L_{cond}\ \text{, where } G = \frac{\dot{m}}{\rho A_{cond}} \tag{12}$$

where friction factor f_{lo} is calculated by Blasius equation $f_{lo} = 0.079\left(\frac{Gd_l}{\mu_l}\right)^{-0.25}$ and the two-phase multiplier ϕ_{lo}^2 is calculate in the following manner: primarily it is determined the flowing state by the Reynolds number calculation to the vapor flowing $Re_v = \frac{\rho_v G x d_v}{\mu_v}$ and also to the liquid flowing $Re_l = \frac{\rho_l G(1-x)d_l}{\mu_l}$, where G is the flow velocity *[m/s]*, x is the quality, μ is the dynamic viscosity *[kg/ms]* and d is tubing diameter *[m]*. Next, it is calculated the Martinelli parameter $X_{tt} = \left(\frac{\rho_v}{\rho_l}\right)^{0.5}\left(\frac{\mu_l}{\mu_v}\right)^{0.125}\left(\frac{1-x}{x}\right)^{0.875}$ and finally the two-phase multiplier $\phi_{lo}^2 = \phi_l^2(1-x)^{1.75}$. Where $\phi_l^2 = 1 + \frac{C}{X_{tt}} + \frac{1}{X_{tt}^2}$ and the constant C is in the Table 2.

Table 2 Constant C to the flowing states of vapor and liquid.

Liquid	Vapor	Flowing State	C
Turbulent	Turbulent	tt	20
Laminar	Turbulent	lt	12
Turbulent	Laminar	tl	10
Laminar	Laminar	ll	5

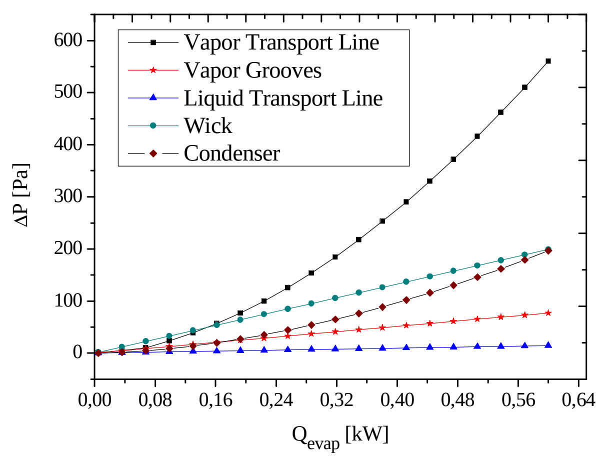

Figure 8. Pressure losses in the capillary pumping system as a function of the input thermal load.

Fig. 8 depicts the pressure losses in the vapor and liquid transport lines, in the grooves, in the condenser and in the wick. All pressure losses are in function of the variation of the heat transfer rate by evaporation into the evaporator, Eq. (13). It is noticed that as the input thermal load increases, the pressure loss in the vapor transport line increases significantly. Because as the thermal load increases, the flowing turbulence increases. On the other hand, for a low thermal load the pressure losses in the wick start to have a larger importance.

The pressure loss in the condenser, according to Maidanik et al. (1991), was considered very small in comparison to the other pressure losses in the system; however, this behavior was not observed in Fig. 8.

4. WORKING FLUID SELECTION

As the capillary pumping systems are two phase loop devices, the working fluid selection is very important for the successful operation. The effects of the sensitive heat in the mass flow rate are only secondary in most case and can be neglected; therefore the mass flow rate can be calculated making an energy balance in the evaporation zone:

$$\dot{Q}_{evap} = \dot{m}\, h_{lv} + \dot{m}\, c_p\, \Delta T_{subcooled} \approx \dot{m}\, h_{lv} \quad \rightarrow \quad \dot{m} = \dot{Q}_{evap} / h_{lv} \tag{13}$$

It is noticed by Eq. (13) that the greater the latent heat, the smaller the mass flow rate and consequently, the smaller the pressure losses.

Varying the water properties, for instance, from the triple point to critical point, as depicted in the Fig 9.

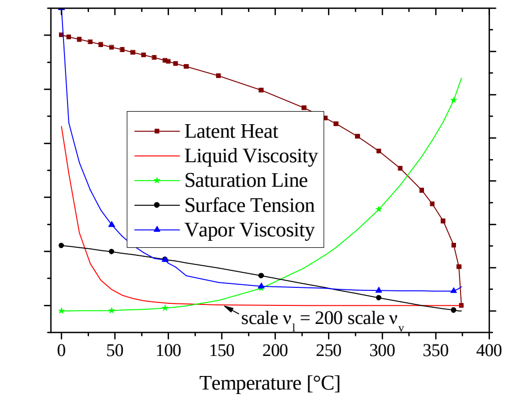

Figure 9. Water properties.

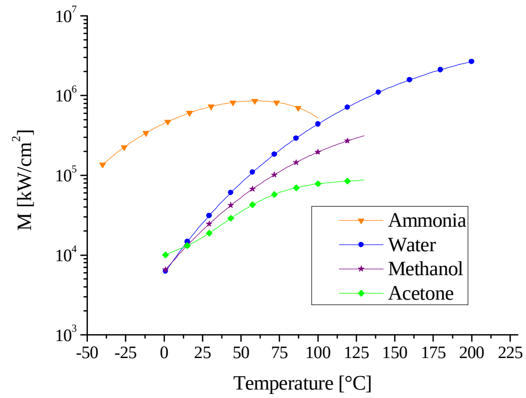

Figure 10. Figure of merit of working fluids for CPL/LHP.

It could be concluded that the proximity of the triple point would be favorable to the capillary pumping system operation. Because in this region are the largest values of vaporization latent heat (leading to smallest mass flow rate and smaller pressure losses in the working fluid flowing) and are the largest values of surface tension (increasing the system pumping capacity). Although the mass flow rate is minimized in the proximity of the triple point, the vapor kinematic viscosity increases exponentially so that is necessary to use larger diameters in the vapor line, in the condenser, as well as in the grooves.

Another way to evaluate and classify the working fluids, in regard to the hydrodynamic efficiency, is made by establishing as a figure of merit, a relationship between the thermophysical properties and geometric factors of the capillary pumping system. In the case of the heat pipes, this figure of merit is obtained through the evaluation of the liquid properties, because in the heat pipes the liquid flowing through the porous structure has the main influence in the total pressure loss of the system. On the other hand, in the CPL and LHP the vapor flowing has the main influence, then a different relationship for the figure of merit, in function of the vapor properties, was obtained by Dunbar and Cadell (1998), mentioned by Maidanik (1999):

$$M = \frac{\rho_v \sigma h_{lv}^{1.75}}{\mu_v^{0.25}} \tag{14}$$

Fig. 10 depicts the figure of merit results (M) for ammonia, water, methanol and acetone. It is noticed that for the temperature range from 0 to 100 °C the best working fluid is ammonia as it was said by Bazzo and Riehl (2003).

In the capillary pumping systems (CPL/LHP) the heat transport can also be limited by the working fluid vapor pressure. It was noticed in the Fig. 11 that in the proximities of the water triple point the pressure decreased. In this temperature range, the vapor pressure can reach smaller values than the maximum capillary pressure head (calculated by Eq. 1), as it can be seen in the Fig. (11a).

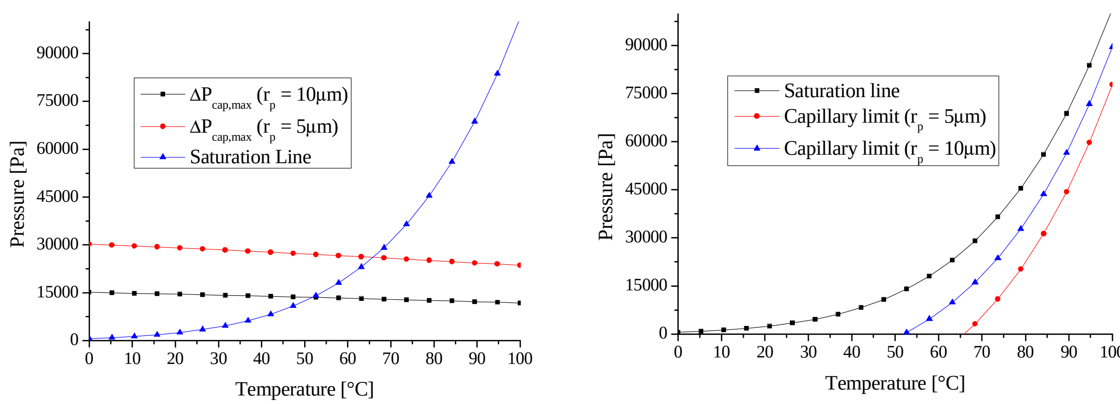

(a) (b)

Figure 11 Vapor absolute pressure and the maximum capillary pressure head (a) and saturation line and capillary limit for pore radius 5 and 10µm (b).

Varying the pore radius it is noticed that the smaller radius, the greater temperature range in which the vapor absolute pressure is smaller than maximum capillary pressure head. In this case, the pressure differential between the vapor and the liquid phase into the meniscus will become the capillary limit. Therefore, in other words, part of the capillary pumping capacity will not be used.

The maximum capillary pressure head is equal to the pressure difference between the liquid and vapor phases in the meniscus ($\Delta P_{cap\,\max} = P_v - P_l$). Since the absolute pressure of the liquid phase cannot be negative, a capillary limit is established when the liquid pressure reaches the abscissas axis, as it can be seen in Fig. (11b). For water, the limit temperature is 52 °C to an effective pore radius 10 μ m and 66 °C for 5 μ m.

According to Ku (1994), the oxygen has been an attractive working fluid for CPLs that work at the temperature below -208 °C. The oxygen vapor pressure at this temperature is 2335 Pa, although the maximum capillary pressure head is 3933 Pa for a pore radius of 10 μ m.

All thermodynamic properties, presented in this paper, were obtained in the Engineering Equation Solver (EES).

5. CONCLUSIONS

Theoretical results concerning a thermohydraulic study in regarding to the designs of CPL and LHP were presented. The PT diagram and the operation modes analyses give precious information to the designers. According to the results, a combined device is recommended to increase the robustness or reliability of the system, besides the operation temperature control flexibility and startup pre-heating. A mathematical model regarding the combined device is under development. Through the analyses done here, the ammonia was the best working fluid for this device that has been manufacturing in the Laboratory of Combustion and Thermal Systems Engineering (LABCET/UFSC). An improved study should be done in the condenser to determine the pressure losses.

6. ACKNOWLEDGMENTS

The authors thank the National Council for Scientific and Technological Development (CNPq), a foundation linked to the Ministry of Science and Technology (MCT) to support Brazilian research.

7. REFERENCES

Bazzo, E. and Riehl, R. R., 2003, “Operation Characteristics of a Small-scale Capillary Pumped Loop”, Applied Thermal Engineering, Vol.23, pp. 687-705.

Carey, V. P., 1992, “Liquid-Vapor Phase-Change Phenomena: An Introduction to the Thermophysics of Vaporization and Condensation Processes in Heat Transfer Equipment, Series in Chemical and Mechanical Engineering”, USA, 639p.

Chernysheva, M. A., Vershinin, S. V. and Maidanik, Y. F., 2007, “Operating Temperature and Distribution of a Working Fluid in LHP”, International Journal of Heat and Mass Transfer, Vol.50, pp. 2704-2713.

Chi, S. W., 1976, “Heat Pipe Theory and Practice”, McGraw-Hill Book Company, Washington, USA, 272p.

Ku, J., 1994, “Thermodynamic Aspects of Capillary Pumped Loop Operation”, Proceedings of the 6th AIAA/ASME Joint Thermophysics and Heat Transfer Conference, AIAA-94-2059, Colorado Springs, USA, pp.1-11.

Ku, J., 1999, “Operating Characteristics of Loop Heat Pipes”, Proceedings of the 29th International Conference on Enviromental System, 1999-01-2007, Denver, Colorado, USA.

Ku, J. and Kroliczek, E. J., 1987, “Analytical Modeling of the Capillary Pumped Loop”, Proccedings of the 6th International Heat Pipe Conference, Grenoble, France, pp. 405-415.

Maidanik, Y. F., Fershtater, Y. G. and Goncharov, K. A., 1991, “Capillary-pump Loop for the Systems of Thermal Regulation of Sapcecraft”, Proceedings of the 4th European Symposium on Space Environmental and Crontrol Systems, Florance, Italy, pp. 87-92.

Maidanik, Y. F., 1999, “State-of-the-art of CPL and LHP Technology”, Proccedings of the 11th International Heat Pipe Conference, Tokyo, Japan, pp. 19-30.

Nikitkin, M. and Cullimore, B., 1998, “CPL and LHP Technologies: What are the Differences, What are the Similarities?”, SAE Paper No. 981587.